Open Access Full Text Article

ORIGINAL RESEARCH

PKCβII-induced upregulation of PGP9.5 and VEGF in postoperative persistent pain in rats

Xiang Zhu*
Yuxi Liu*
Hongfang Huang
Yonghua Zhang
Saisai Huang
Weiwei Zhou
Xiaocui Bian
Shiren Shen
Su Cao

Department of Anesthesiology, Affiliated Hospital of Nantong University, Nantong, Jiangsu 226001, People's Republic of China

*These authors contributed equally to this work

Purpose: Postoperative pain is a common clinical problem. In this study, we aimed to investigate the role of protein kinase C βII (PKCβII) in the progression of postoperative pain following skin/muscle incision and retraction (SMIR) surgery.

Materials and methods: SMIR postoperative pain model was established in rats, akin to a clinical procedure. The expression level and location of p-PKCβII were observed in dorsal root ganglion (DRG) or spinal cord from SMIR-operated rats by Western blotting and immunofluorescence. In addition, the effects of PKCβII on the expression of protein gene product 9.5 (PGP9.5) or vascular endothelial growth factor (VEGF) were assessed by using pharmacological activator and inhibitor of PKCβII. Moreover, mechanical withdrawal threshold (MWT) was assessed before or after SMIR-operated rats were treated with inhibitor or activator of PKCβII.

Results: The expression of PKCβII in DRG and spinal cord was significantly increased after SMIR surgery ($P < 0.001$, $P < 0.01$) and expression of PKCβII was located in the neurons of the spinal cord, and magnocellular neurons, non-peptide neurons, and peptide neurons in DRG. Besides, compared with skin/muscle incision group, retraction caused a marked increase in the expression of PKCβII and a significant decrease of MWT ($P < 0.001$, $P < 0.05$). The activator of PKCβII greatly increased the expression of PGP9.5 and VEGF ($P < 0.05$, $P < 0.01$) and enhanced MWT ($P < 0.001$), while inhibitor of PKCβII decreased the expression of PGP9.5 and VEGF and attenuated MWT ($P < 0.05$, $P < 0.01$, $P < 0.001$).

Conclusion: Activation of PKCβII signaling pathways might be an important mechanism in the progression of postoperative pain.

Keywords: postoperative persistent pain, neurons, PKCβII, PGP9.5, VEGF

Introduction

Postoperative pain is a common clinical problem encountered by about 10–50% of patients. With extinction of postoperative inflammation or tissue healing, it may develop from acute pain to chronic persistent pain.[1] Consequently, the mechanism underlying the transformation from acute pain to chronic persistent pain after surgery becomes an important research field which has been extensively studied. Most studies focused on peripheral sensitization and central sensitization caused by neuronal plasticity.

Protein kinase C (PKC) isozymes are a family of serine/threonine protein kinases that are divided into three subfamilies based on structural differences in their amino-terminal regulatory domains.[2] The conventional PKC isozymes include the isoforms α, βI, βII, and γ, which are sensitive to activation by diacylglycerol, phorbolesters, and

Correspondence: Yuxi Liu; Dr Su Cao
Department of Anesthesiology, Affiliated Hospital of Nantong University, 20 Xisi Road, Nantong, Jiangsu 226001, People's Republic of China
Email liuyuxi919@163.com; su1_cao123@163.com

calcium. Among them, PKCβII is an alternatively spliced isoform of PKCβI which contains an additional 43 residues at the amino terminus.

PKC plays very wide and important functions in various phenomena of life, which can induce pain in a variety of ways.[3–5] Besides, its blockers have been shown to enhance the analgesic effect of morphine.[6] Moreover, high expressed PKC is also observed to have an effect on mitochondrial function,[7] cell injury and apoptosis,[8,9] cell adhesion,[10] and astrocytes gap junction protein.[11] In addition, increased expression of PKC isoform is associated with neuronal plasticity and the release of neurotransmitters.[12] Interestingly, a number of PKC isozymes (α, βI, and βII; calcium-dependent) have been found in the anatomical areas that regulate chronic pain and nociception (e.g., amygdala, periaqueductal gray, dorsal root ganglia, spinal cord, etc.), but individual subtype is not necessary for acute pain.[13] Yet studies regarding the mechanisms of postoperative pain, in response to PKC isozymes, are scarce. Thus, uncertainty remains regarding the direct effects of PKCβII on nociceptors.

In the present study, we established the rat model of postoperative pain evoked by skin/muscle incision and retraction (SMIR) surgery according to reference by Flatters.[14] We aimed to study alterations of PKCβII expression after SMIR, to investigate the role of PKCβII on the progression of postoperative persistent pain following SMIR surgery.

Materials and methods
Animals and grouping
Male adult Sprague Dawley rats (weighing 200–250 g) were purchased from the Experimental Animal Center of Nantong University (Jiangsu, China) and maintained in the animal housing facility with controlled room temperature ($23 \pm 1^\circ$C) and allowed free access to rodent diet and tap water. The rats were acclimatized to the housing facility for 3 days before experiments. In this study, all the experimental protocols were approved by the Animal Use and Care Committee for Research and Education of Nantong University (Jiangsu, China). Animal treatments were performed according to the Guidelines of the International Association for the Study of Pain.[15]

The rats were randomly assigned to six groups (n = 5/group): control group, Sham group, SMIR group, PKCβII agonist group, PKCβII Inhibitor group, and solvent group. The rats in the control group did not receive any treatment. Sham-operated rats underwent skin/muscle incision with the exception of the skin/muscle retraction. The rats in the SMIR group underwent 1-h retraction after the skin/muscle incision as described by Flatters.[14] PKCβII agonist TPA, Phorbol

12-myristate 13-acetate (PMA) (110 ng; Sigma-Aldrich Co., St. Louis, MO, USA; lot number: P8139-1MG) and PKCβII inhibitor LY333351 (20 µg; Enzo Life Sciences; lot number: ALX-270-348-M001) were dissolved in 0.25% DMSO (Sigma-Aldrich Co.; lot number: S16063) and were intrathecally injected into animals of PKCβII agonist and PKCβII inhibitor groups, respectively, on 7th day after SMIR surgery, while rats in solvent group were injected with 0.25% DMSO. For intrathecal injection, the rats were anesthetized with isoflurane. The spinal cord puncture was made with a 30-gauge needle between the L4 and L5 level to deliver the reagents (20 µL) to the cerebrospinal fluid. Immediately, a brisk tail flick was observed after the needle entry into the subarachnoid space.[16]

Establishment of theSMIR model
The animals were anesthetized with 10% chloralhydrate (400–500 mg/kg, intraperitoneal) and placed in the supine position. A 1.5–2 cm skin incision, 4 mm medial to the saphenous vein, was made to expose the muscle of the thigh, after the medial thigh on the right leg was shaved and sterilized. An incision (7–10 mm long, 4 mm medial to the saphenous nerve) was made in the superficial muscle layer of the thigh. To allow the insertion of a micro-dissecting retractor, the superficial muscle was then isolated by spreading blunt scissors within the muscle incision site. The retractor was inserted into the incision site, and the superficial muscle of the thigh was retracted by 2 cm. During the retraction period, the saphenous nerve was displaced and potentially stretched around the retractor, but not compressed against a hard surface such as bone. The incision site was covered with gauze that was moistened with sterile saline to prevent surgical site dehydration. After 1 h, the muscle and skin of the surgical site was closed with 4.0 Vicryl ® (Ethicon US, LLC, Bridgewater, NJ, USA) sutures.

Measurement of mechanical allodynia
Mechanical allodynia was assessed using up-down paradigm[17] with von Frey filaments (IITC Life Science Inc. Woodland Hills, CA, USA) ranging from 1.4 to 26 g. Animals were placed on an elevated wire mesh floor and confined underneath individual overturned Plexiglass® box (Nantong Jingxin Optical Glass, Co. Ltd., Nantong, China) ($22 \times 22 \times 12$ cm^3). Before baseline (preoperative) recording, rats were adapted to the testing environment, 30 min/d for 3 consecutive days. Tests were conducted from 8:30 a.m. A series of von Frey hair stimuli was delivered in an ascending order of forces to the mid-plantar area of the hind paw encircled by tori/footpads. Shrinking, swing, or paw licking were regarded

as positive reactions. Each filament was presented five times within 30 s to determine the response threshold. If the response was not elicited at least twice, the next ascending von Frey filament was applied until at least two responses were observed. The responses were recorded in grams of paw withdrawal averaged over 3–5 applications referred to as mechanical withdrawal threshold (MWT). Behavioral tests were performed prior to and 1, 3, 7, 14, and 21 days following SMIR surgery.

Measurement of thermal allodynia

Animals were placed in individual Perspex boxes on a glass floor. Nociceptive responses to a noxious heat stimulus were examined by measuring the hind paw withdrawal latency from a focused beam of radiant heat to the plantar surface using a plantar test apparatus (Ugo Basile, Milan, Italy). The apparatus had a built-in cut-off latency of 31.2 s and evoked hand paw withdrawal latencies of 12–14 s when the light intensity was set at 40 W. Right hind paw of each rat was tested three times and then an average of these three readings was taken. To avoid sensitization of the paws, a gap of 5 min was given before the same hind paw was retested. Prior to the SMIR procedure, three baseline measurements of heat sensitivity were taken on separate days, and the averaged value was taken as pre-surgery baseline value.

Western blotting

After the rats were anesthetized as described previously, lumbar regions 3–5 of the spinal cord and L5 DRG were prepared in the same manner at appropriate survival times and homogenized in a lysis buffer containing protease and phosphatase inhibitors (Sigma-Aldrich Co.). Protein concentrations were measured by the BCA Protein Assay (Pierce, Rockford, IL, USA). Subsequently, equal amounts (40 μg/lane) of total protein from the spinal cord sample and equal amounts (30 μg/lane) of total protein from DRG sample were separated on 10% SDS-PAGE (Beyotime Biotech Inc., Nanjing, China) and transferred onto polyvinylidene difluoride membranes using standard procedures. The membranes were blocked with 5% milk in phosphate-buffered saline (PBS) with 0.1% Tween-20 for 120 min at room temperature. Following washes, blots were incubated overnight at 4°C with polyclonal antibody against PKCβII phosphorylated on Ser660 (rabbit, 1:200; Abcam), VEGF (sheep, 1:200; sc-7903; Santa Cruz Biotechnology, Inc., Dallas, TX, USA), PGP9.5 (mouse, 1:200; Abcam). For the loading control, glyceraldehyde phosphate dehydrogenase (GAPDH) antibody (mouse, 1: 20,000; EMD Millipore, Billerica, MA, USA) served as an

endogenous internal reference. The membranes were washed three times with Tris-buffered saline/Tween buffer and incubated with the corresponding horseradish peroxidase-conjugated secondary antibody (1:2,000; GE Healthcare Life Sciences, Chalfont, UK) for 2 h followed by three washes. Blots were visualized in electrochemiluminescence solution and exposed on Hyperfilm (Bio-Rad Laboratories Inc., Hercules, CA, USA) for 2–5 min. Specific bands were then evaluated by apparent molecular size. The intensity of the selected bands was analyzed by using Image J software (NIH, Bethesda, MD, USA).

Immunohistochemistry

On day 0 and day 7 after SMIR, the rats were anesthetized with pentobarbital and perfused through the ascending aorta with PBS followed by 4% paraformaldehyde in 0.1 M PB. After the perfusion, the L3–L5 spinal cord and L5 DRG from each rat were quickly removed, post-fixed in the same fixative at 4°C overnight and transferred to 20% and subsequently in 30% sucrose solution, respectively. After cryoprotection with 30% sucrose, the spinal cord (30 μm, free-floating) and DRG sections (14 μm) were cut in a cryostat and processed for immunofluorescence staining. The sections were first blocked with 5% goat serum for 2 h at room temperature and then incubated at 4°C overnight with the following primary antibodies: PKCβII phosphorylated on Ser660 (rabbit, 1:200; Abcam), NeuN antibody (mouse, 1:5,000; EMD Millipore), CD11-b (mouse, 1:200; EMD Milipore), and glial fibrillary acidic protein (GFAP) antibody (mouse, 1:5,000; EMD Millipore) for spinal cord and NF200 (mouse, 1: 1,000; EMD Milipore), IB4 (mouse, 1:6,000; Sigma-Aldrich Co.), and calcitonin gene-related peptide (CGRP) (mouse, 1:1,000; Sigma-Aldrich Co.) for DRG section. The sections were then incubated for 2 h at room temperature with Cy3- or fluorescein isothiocyanate (FITC)-conjugated secondary antibodies (1:400; Jackson ImmunoResearch, West Grove, PA, USA). For double immunofluorescence, the sections were incubated with a mixture of mouse and rabbit (or goat) primary antibodies followed by a mixture of FITC- and Cy3-conjugated secondary antibodies. The stained sections were examined with a Leica fluorescence microscope, and images were captured with a charge-coupled device (CCD) spot camera. The sections with double staining were imaged with an FV10i confocal microscope (Olympus, Tokyo, Japan).

Statistical analysis

All statistical analyses were presented as mean ± SEM and analyzed by SPSS 16.0 software (SPSS Inc., Chicago, IL,

USA). For behavioral studies, the data were analyzed with two-way analysis of variance (ANOVA) followed by a Bonferroni's test for post hoc analysis. The differences of protein expression among multiple groups were compared by using one-way ANOVA followed by Newman–Keuls post hoc test or by the Student's t-test if only two groups were applied. $P < 0.05$ was considered statistically significant.

Results
SMIR surgery induces MWT values
Before investigating mechanical pain, we performed experiments to investigate whether SMIR affects heat hyperalgesia. As shown in Figure 1A, SMIR had no effects on heat hyperalgesia or cold allodynia pain hypersensitivity, which is consistent with previous report.[18] Therefore, mechanical hypersensitivity became the focus. As shown in Figure 1B, the MWT was obviously decreased at each time point in the SMIR group compared to the control and sham-operated group in a time-dependent manner ($P < 0.05$, $P < 0.01$, $P < 0.001$, respectively). The MWT of SMIR-operated rats decreased on postoperative day 1 and this decrease was held on for over 21 days. During the period of SMIR-induced mechanical hypersensitivity in the ipsilateral paw, the postoperative day 7 showed the most prominent reduction (the threshold decreased by 86%) compared with the baseline ($P < 0.001$). However, the sham-operated and normal groups did not show any marked changes at any of the time points, and no significant difference was observed between the Sham and normal groups ($P > 0.05$). The results indicated that SMIR induced persistent significant mechanical hypersensitivity, in a time-dependent manner.

SMIR induces p-PKCβII expression in the spinal cord and in DRG
According to the time course of SMIR-induced pain behavior, we examined p-PKCβII expression in the lumbar spinal cord and DRG (L4–5) at 7 days after SMIR by using Western blotting and immunostaining in naïve, sham, and SMIR-operated groups. Western blot analysis showed that p-PKCβII expression significantly increased at day 7 after SMIR both in the lumbar spinal cord ($P < 0.05$, SMIR vs naïve, sham; Figure 2A) and in the DRG ($P < 0.05$, SMIR vs naïve, sham; Figure 3A). Immunohistochemistry showed that p-PKCβII was expressed in the superficial dorsal horn. More p-PKCβII-immunoreactive (IR) cells were found in SMIR-operated rats than in naïve and sham rats at postoperative day 7 in the spinal cord ($P < 0.05$, Figure 2B and C) and in the DRG ($P < 0.05$, Figure 3B and C).

To define the cellular distribution of p-PKCβII in the spinal cord, we performed double staining of p-PKCβII with different cell markers. As shown in Figure 4, p-PKCβII-IR was colocalized with the neuronal marker NeuN (Figure 4C), but not with microglial marker CD11b (Figure 4F) or astrocytic marker GFAP (Figure 4I), suggesting the localization of p-PKCβII is in spinal neurons.

In addition, the cellular distribution of p-PKCβII in DRG was also determined by double staining of p-PKCβII with different cell markers. As shown in Figure 5, p-PKCβII-IR was colocalized mostly with the non-peptide neuron marker IB4 (Figure 5F), but slightly with magnocellular neurons marker NF200 (Figure 5C) or peptide neuron marker CGRP (Figure 5I), suggesting the localization of p-PKCβII in magnocellular neurons, non-peptide neurons, and peptide neurons in DRG, but mostly in the non-peptide neurons.
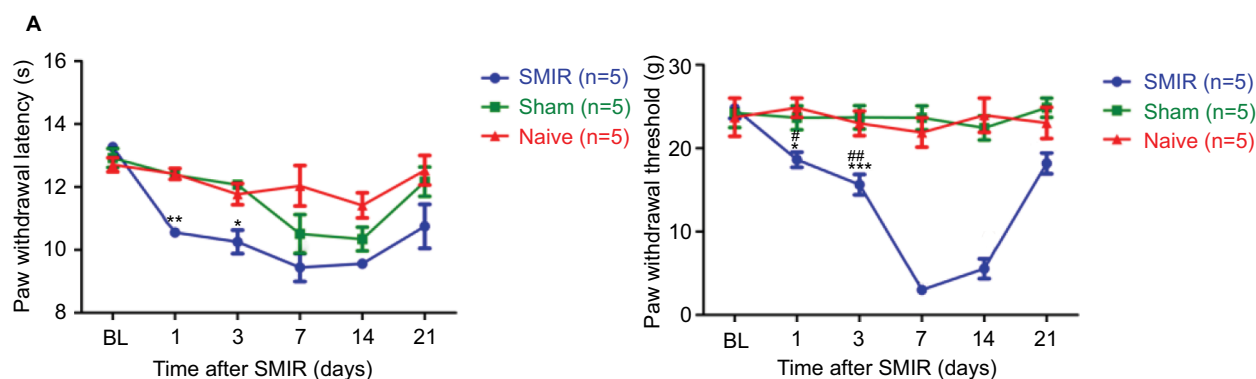

Figure 1 (**A**) Skin/muscle incision and retraction (SMIR)-induced thermal response to pain. Compared with the control group, #$P < 0.05$; compared with the Sham group, *$P < 0.05$, **$P < 0.01$. (**B**) SMIR-induced allodynia (mechanical pain sensitization) in response to hind paw mechanical stimulation. The mechanical withdrawal thresholds (MWTs) in the control (naïve), sham, and SMIR groups are plotted at baseline and at different time points after SMIR. The decreased MWT after SMIR is indicative of allodynia. Compared with the control (naïve) group, #$P < 0.05$, ##$P < 0.01$, ###$P < 0.001$; compared with the Sham group, *$P < 0.05$, ***$P < 0.001$.
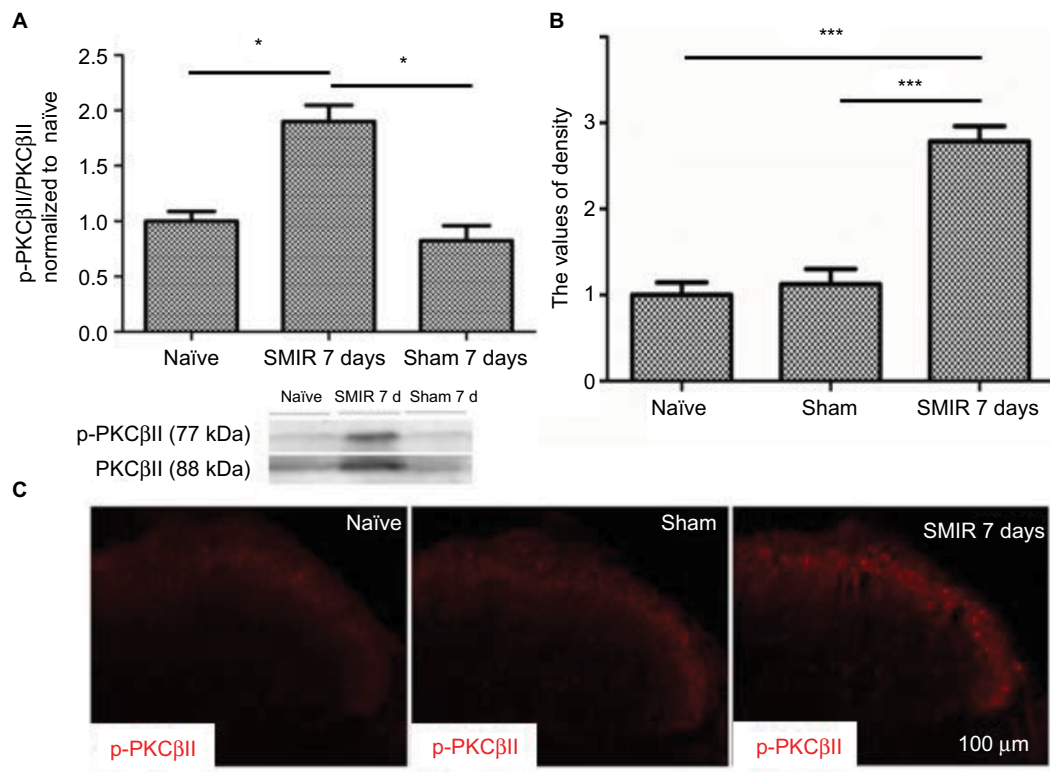
Figure 2 Upregulation of p-PKCβII in the lumbar spinal cord after SMIR. (**A**) Expression of p-PKCβII 7 days after SMIR was determined by densitometric analysis on Western blots using PKCβII as control. Compared with the untreated control and Sham groups, expression level of p-PKCβII was significantly higher at 7 days after SMIR (*$P < 0.05$); n=5 for each group. (**B**) Average values of density of p-PKCβII-positive cells in the lumbar spinal cord in SMIR, naïve, and Sham groups. SMIR and Sham values were compared for the same time and segment by one-way analysis of variance (***$P < 0.001$); n=5 for each group. (**C**) Immunostaining pictures of the p-PKCβII expression in the lumbar spinal cord in naïve, sham, and SMIR 7 days animals.
Abbreviations: SMIR, skin/muscle incision and retraction; PKCβII, protein kinase C βII.

Intrathecal injection of PKCβII agonist PMA enhances mechanical allodynia

To investigate the role of PKCβII in the mechanical allodynia, we intrathecally injected a PKCβII agonist PMA at a dose of 100 ng at day 7 after SMIR. As shown in Figure 6, the MWT was obviously decreased in the PMA group, as compared with the solvent group and the naïve group, in a time-dependent manner. The MWT of PMA rats was significantly decreased at 1 h after injection, and this decrease was held on for about 6 h ($P < 0.001$). Afterward, the MWT began to recover to the baseline level, and after 12 h PMA did not show any effect on mechanical allodynia ($P > 0.05$). This result suggested that PKCβII activation aroused mechanical allodynia.

PMA upregulates PGP9.5 and VEGF expression

To examine whether PGP9.5 and VEGF are involved in neuropathic pain, we then tested the PGP9.5 and VEGF expression level after PMA treatment. The results indicated

that PMA upregulated the PGP9.5 and VEGF expression both in the spinal cord (Figure 7A and B) and DRG (Figure 7C and D) significantly ($P < 0.05$, $P < 0.01$, $P < 0.001$).

Intrathecal injection of PKCβII inhibitor LY333531 attenuates mechanical allodynia

Further, we determined whether the PKCβII inhibitor was capable of reducing allodynia. As the MWT peaks at 7 days after SMIR, we examined the analgesic effect of the PKCβII inhibitor LY333531 by intrathecal injection at 7 days after SMIR. As shown in Figure 8, intrathecal injection of LY333531 markedly increased MWT initiation within 1 h and peaked at 6 h ($P < 0.01$, $P < 0.001$), with the pain returning within 12 h ($P > 0.05$).

LY333531 downregulates PGP9.5 and VEGF expression

To determine the possible role of PGP9.5 and VEGF in LY333531-induced inhibition of neuropathic pain, we
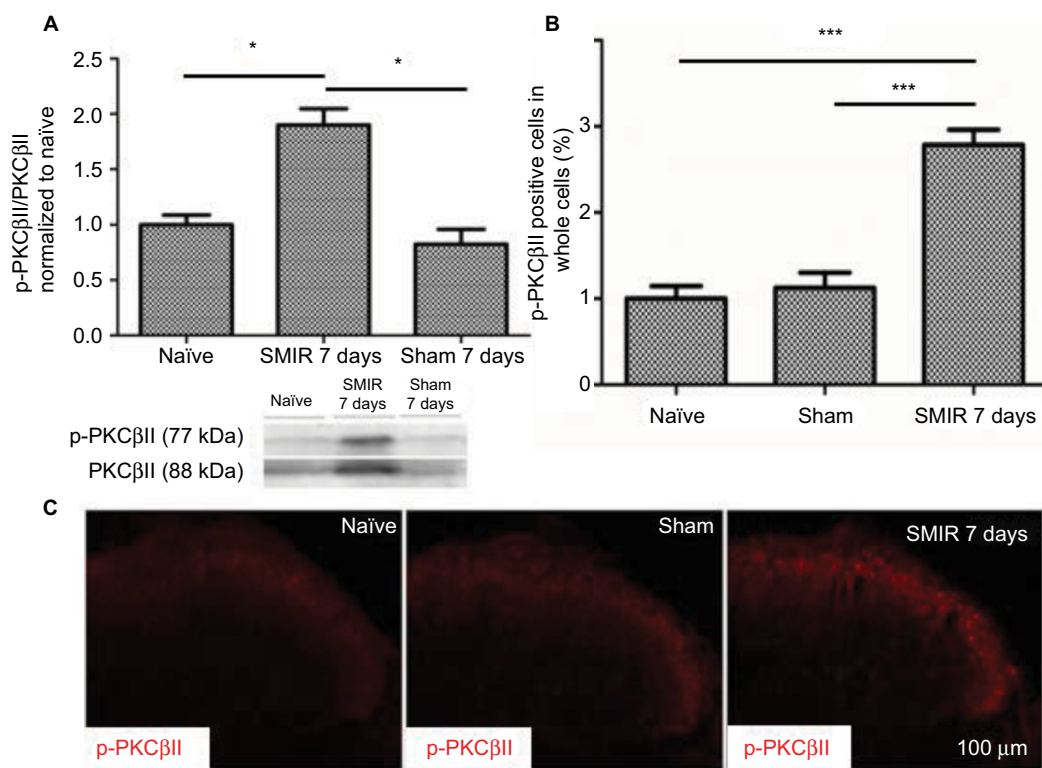
Figure 3 Upregulation of p-PKCβII in the DRG after SMIR. (**A**) Expression of p-PKCβII 7 days after SMIR was determined by densitometric analysis on Western blots using PKCβII as control. Compared with the untreated control and Sham groups, expression levels of p-PKCβII were significantly higher 7 days after SMIR (*$P < 0.05$); n=5 for each group. (**B**) Average values (SD) of densitometric analysis of p-PKCβII-positive cells in the DRG in SMIR, naïve, and sham groups. SMIR and Sham values were compared for the same time and segment by one-way analysis of variance (***$P < 0.001$); n=5 for each group. (**C**) Immunostaining pictures of the p-PKCβII expression in the DRG in naïve, sham, and SMIR animals.
Abbreviations: SMIR, skin/muscle incision and retraction; DRG, dorsal root ganglion; PKCβII, protein kinase C βII.
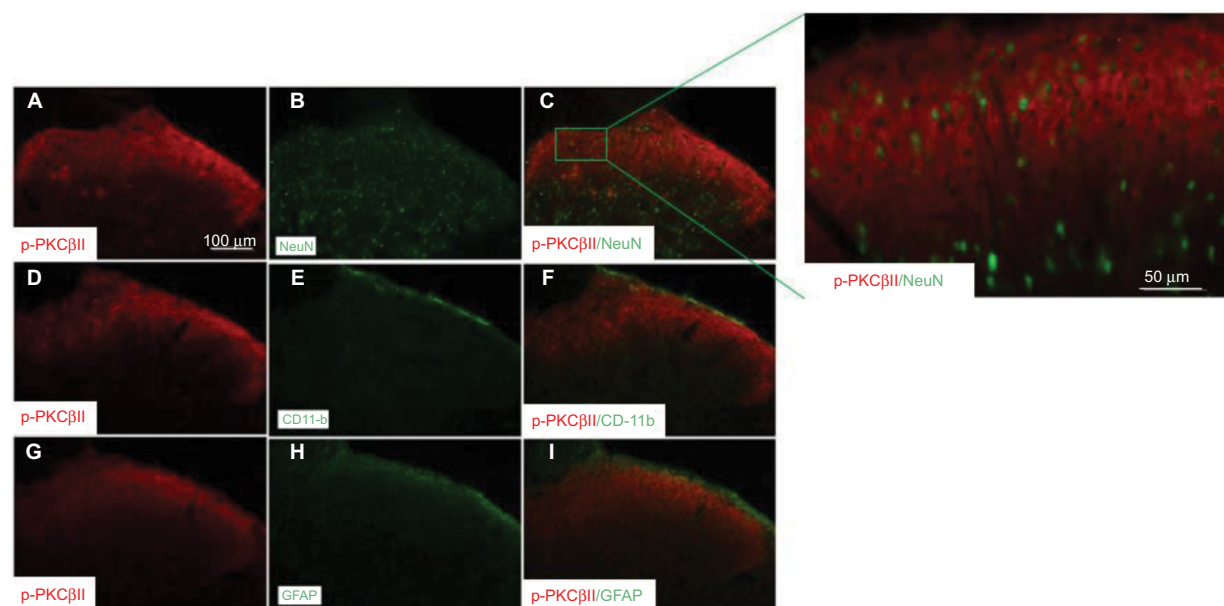

Figure 4 Neuronal expression of p-PKCβII in the lumbar spinal cord. Spinal cord sections (L4–L5) excised 7 days after SMIR were double-labeled with p-PKCβII and the neuron marker (NeuN) (**A–C**) antibodies, or p-PKCβII and microglial marker (CD11b) (**D–F**) antibodies, or p-PKCβII and glial fibrillary acidic protein (GFAP) (**G–I**) to detect the expression of p-PKCβII. Double staining shows that p-PKCβII is co-localized with NeuN, but not with CD11b or GFAP.
Abbreviations: SMIR, skin/muscle incision and retraction; PKCβII, protein kinase C βII.
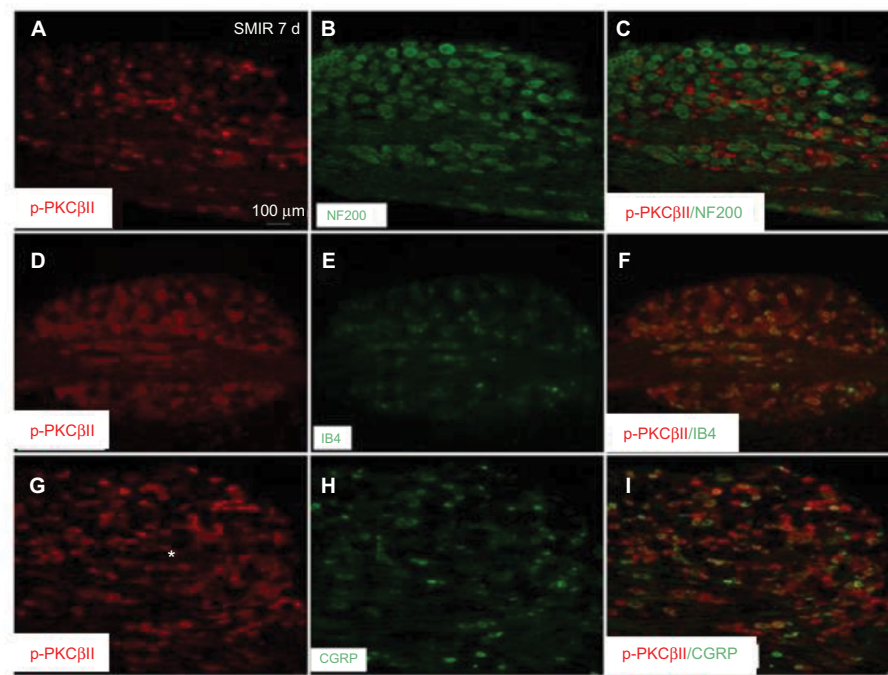
Figure 5 Expression of p-PKCβII in the L5 DRG in SMIR, naïve, and Sham groups. L5 DRG sections excised 7 days after SMIR were double-labeled with p-PKCβII and DRG magnocellular neurons marker (NF200) antibodies (**A–C**), or p-PKCβII and DRG non-peptide neuron marker (IB4) antibodies (**D–F**), or p-PKCβII and DRG peptide neuron marker (CGRP) antibodies (**G–I**) to detect the expression of p-PKCβII. Double staining shows that p-PKCβII is colocalized with NF200 (**C**), IB4 (**F**), and CGRP (**I**).
Abbreviations: SMIR, skin/muscle incision and retraction; DRG, dorsal root ganglion; CGRP, calcitonin gene-related peptide; PKCβII, protein kinase C βII.
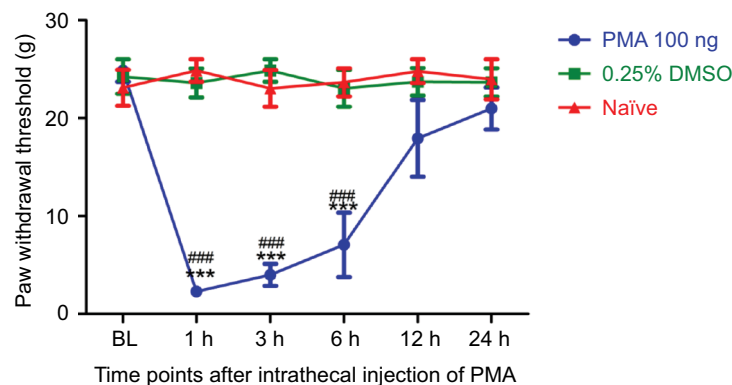

Figure 6 At day 7 after SMIR, intrathecal injection of p-PKCβII agonist PMA at a dose of 100 ng increases mechanical allodynia. Compared with the 0.25% DMSO group, ***$P < 0.001$; compared with the control group, ###$P < 0.001$; n=5 for each group.
Abbreviations: SMIR, skin/muscle incision and retraction; PKCβII, protein kinase C βII; PMA, TPA, Phorbol 12-myristate 13-acetate; BL, baseline.

then tested the PGP9.5 and VEGF expression levels after LY333531 (20 µg) treatment at 7 days after SMIR. The results indicated LY333531 significantly reduced SMIR-induced PGP9.5 and VEGF expression both in the spinal cord (Figure 9A and B) and in the DRG (Figure 9C and D) ($P < 0.05$, $P < 0.01$, $P < 0.001$).

Discussion

SMIR, which stretches skin/muscle tissue around the incision without damaging the main peripheral nerves, can better reflect the characteristics and postoperative persistent pain around the incision process of inflammatory microenvironment.[14] SMIR in rats resulted in prolonged allodynia, confirming the utility of this model of postoperative pain. In this study, we used SMIR model made in the thigh of rats to study the effect of PKCβII on the mechanisms of progression from acute to chronic pain. Naïve, sham-operated, and SMIR animals were evaluated for pain progression with measurements of mechanical allodynia developed in the plantar surface of the respective hind paws. Results show that MWT of SMIR
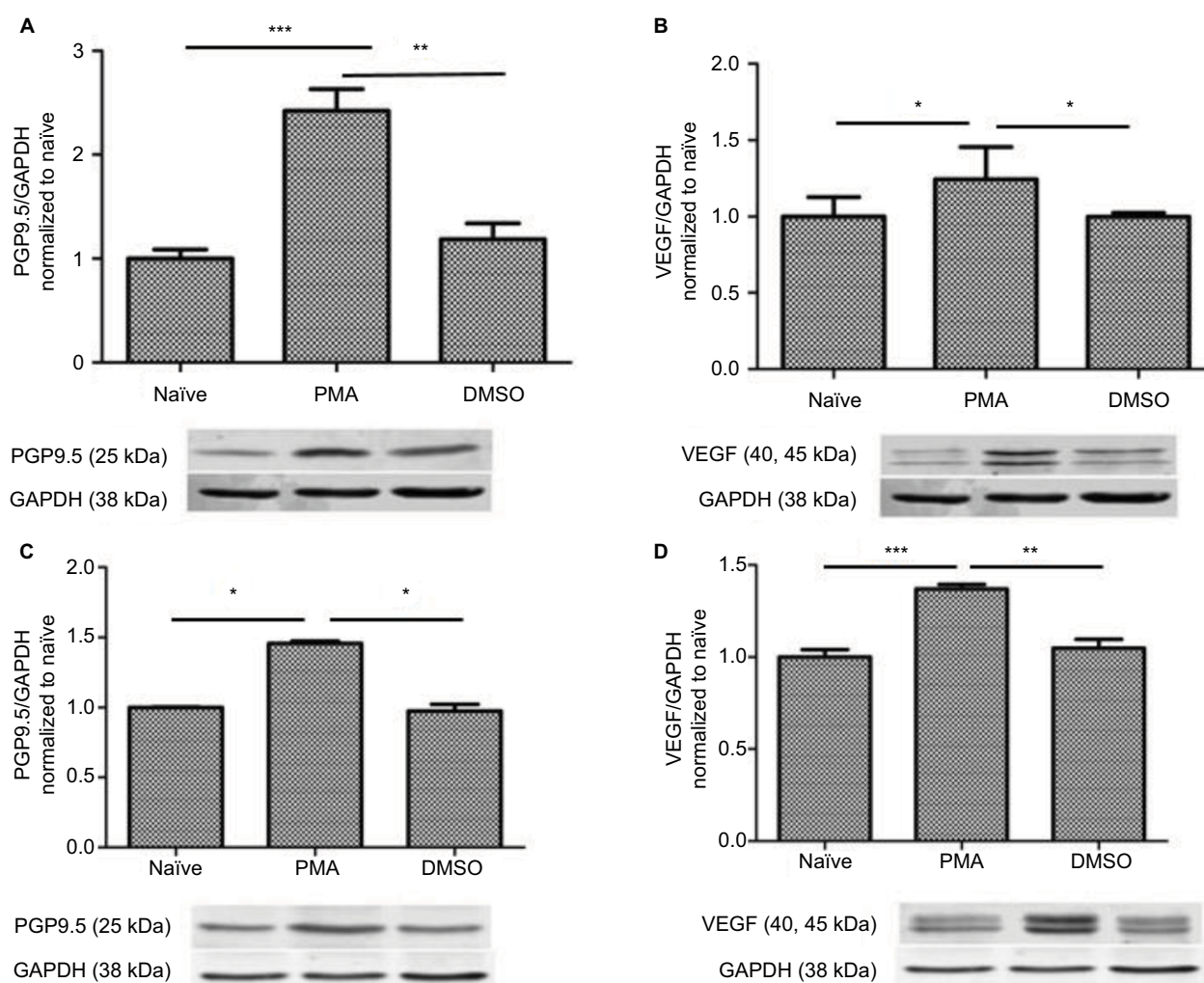
Figure 7 Upregulation of PMA-induced PGP9.5 and VEGF expression in the spinal cord and the DRG. (**A, B**) Expression of PGP9.5 and VEGF in the spinal cord after PMA treatment was determined by densitometric analysis on Western blots using GAPDH as the internal control. Compared with the control and DMSO group, *$P < 0.05$, **$P < 0.01$, ***$P < 0.001$; n=5 for each group. (**C, D**) Expression of PGP9.5 and VEGF in the DRG after PMA Treatment was determined by densitometric analysis on Western blots using GAPDH as the internal control. Compared with the control and DMSO group, *$P < 0.05$, **$P < 0.01$, ***$P < 0.001$; n=5 for each group.
Abbreviations: DRG, dorsal root ganglion; PGP, protein gene product; PGP9.5, protein gene product 9.5; VEGF, vascular endothelial growth factor; PMA, TPA, Phorbol 12-myristate 13-acetate.

rats decreased in a time-dependent manner and these changes might be related with PKCβII. Immunostaining suggested that p-PKCβII was associated with neurons, but not with microglia or astrocytes in lumbar spinal cord slices and associated with DRG non-peptide neurons, as well as slightly associated with magnocellular and CGRP-containing neurons. Importantly, we found the PKCβII agonist PMA could enhance mechanical allodynia, while its inhibitor, LY333531, reversed and lowered the pain due to allodynia at the 7th day of SMIR. Further studies suggested that the role of PKCβII in regulating mechanical allodynia is related with PGP9.5 and VEGF.

As shown in Figure 1, the MWT of SMIR decreased significantly, and this decrease was held on for over 21 days.

The decrease of MWT reached the peak at the postoperative day 7, demonstrating SMIR induced mechanical allodynia. Western blot showed the p-PKCβII protein expression level in the SMIR group, 7 days after surgery, was significantly higher compared with that in the normal group and Sham group, in the spinal cord and the DRG. This result may indicate that persistent postoperative pain induced the activation of PKCβII. We speculated that the surgical operation method influenced mechanical hypersensitivity and the expression of p-PKCβII: stretching skin and muscle in SMIR group increased mechanical hypersensitivity and expression level of PKCβII more significantly than simple incision of skin and muscle.
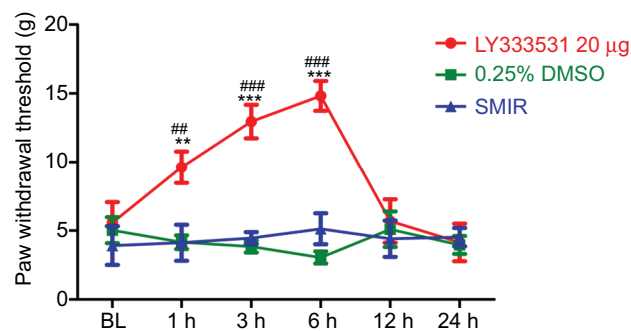
Figure 8 Intrathecal injection of p-PKCβII inhibitor LY333531, at 7 days after SMIR, reverses SMIR-induced mechanical allodynia. Compared with the 0.25% DMSO group, **$P < 0.01$, ***$P < 0.001$; Compared with the SMIR group, ##$P < 0.01$, ###$P < 0.001$; n=5 for each group.
Abbreviations: SMIR, skin/muscle incision and retraction; BL, baseline.

PKCβII is sensitive to activation by calcium, expressing in sensory neurons of mice.[19] Our immunohistochemistry results showed that p-PKCβII was co-localized with neurons in the spinal cord and was co-localized primarily with non-peptide neurons, and in a small amount with magnocellular neurons and peptide neurons in DRG. Peptide nerve fibers are neuropeptides, for example, CGRP, prompting abnormal increase of neuronal excitability,[20,21]associated with non-damaging information. Non-peptide nerve fibers are dependent on glial cell-derived neurotrophic factor,[22] which is associated with damaging information. Nerve axon plays an important role in a series of pathophysiological changes (functions of neurons, the regeneration of nerve fibers and
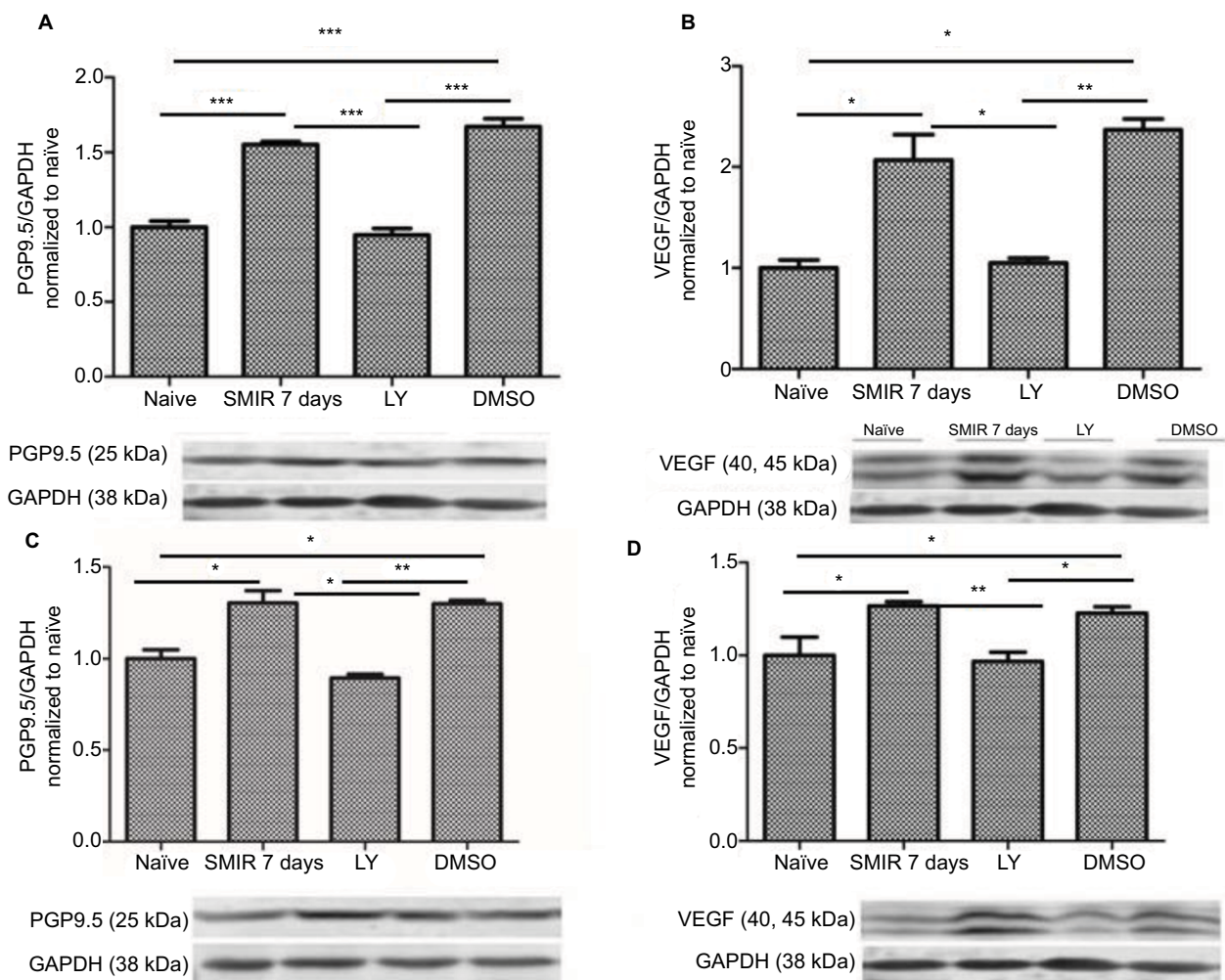

Figure 9 Downregulation of LY333531-induced PGP9.5 and VEGF expression in the spinal cord and the DRG. (**A, B**) Expression of PGP9.5 and VEGF in the spinal cord after LY333531 treatment was determined by densitometric analysis on Western blots using GAPDH as the internal control. Compared with the control and DMSO group, *$P < 0.05$, **$P < 0.01$, ***$P < 0.001$; n=5 for each group. (**C, D**) Expression of PGP9.5 and VEGF in the DRG after LY333531 treatment was determined by densitometric analysis on Western blots using GAPDH as the internal control. Compared with the control group, LY group, and DMSO group, *$P < 0.05$, **$P < 0.01$; n=5 for each group.
Abbreviations: SMIR, skin/muscle incision and retraction; DRG, dorsal root ganglion; VEGF, vascular endothelial growth factor; GAPDH, glyceraldehyde phosphate dehydrogenase; LY, LY333531; PGP, protein gene product.

axoplasmic transport, etc.).[23] Collectively, the results of the present study confirmed that the activation of PKCβII may play an important role in the postoperative persistent pain through affecting postoperative changes of neuron pathophysiological process (inflammation, metabolism, damage/repair, information transmission, etc.).

PKCβII inhibits cell apoptosis[24] by regulating glucose and repairing damaged cell migration.[25] PGP9.5 is the special ubiquitin hydroxyl hydrolytic enzyme in nerve fibers, a nerve-specific marker.[26,27] The increasing or decreasing of its expression represents the process of the nerve repair or damage, respectively.[28] Previous findings have shown that inflammation and pain process (for example, fracture, tumor, infection, etc.) can upregulate the PGP9.5 expression.[29–32] VEGF promotes the blood vessels, increases vascular permeability,[33] increases glucose levels in the cell by PKC,[34] promotes energy metabolism,[35] protects nerve cells,[36] and reflects the body's ability to repair.[35] An increased VEGF protein expression level has previously been found to induce an inflammatory response and promote the release of algogenic substances.[37] In the present study, the rats that were treated with PKCβII agonist PMA showed enhanced mechanical allodynia, and PGP9.5 and VEGF levels were upregulated both in the spinal cord and in the DRG. These results suggested that activation of p-PKCβII induced postoperative pain by upregulating PGP9.5 and VEGF expression. Additionally, spinal administration of PKCβII inhibitor LY333531 markedly decreased the severity of mechanical allodynia, and PGP9.5 and VEGF were downregulated in the spinal cord and the DRG. The results confirmed that inhibition of PKCβII downregulated PGP9.5 and VEGF expression to alleviate postoperative pain. Our findings from these experiments emphasize that PKCβII plays an essential role in the relief of postoperative chronic pain condition and verified that PGP9.5 and VEGF were involved in central sensitization and mechanical hypersensitivity in acute and persistent pain status. So, in the repair course of tissue and neuron, activation of the expression of PKCβII affects pain signaling through its effects on upregulating both PGP9.5 and VEGF, to provide positive energy for cell intrinsic growth, promote axonal growth, for regeneration and sensitization pathways, and thus promote postoperative persistent pain (Figure 10).

In conclusion, our study demonstrated that SMIR induced mechanical allodynia and activated PKCβII signaling pathways Therefore, downregulation of PKCβII could be a viable treatment strategy for relieving of postoperative pain. Our present study provides new data by demonstrating both molecularly (by Western blotting) and immunologically (by immunohistochemistry), following 7 days of SMIR, the upregulation of PKCβ (p-PKCβ2/PKCβ2) in the DRG and lumbar spinal cord, and the main pathways involved in pain coming from the periphery to the central nervous system.
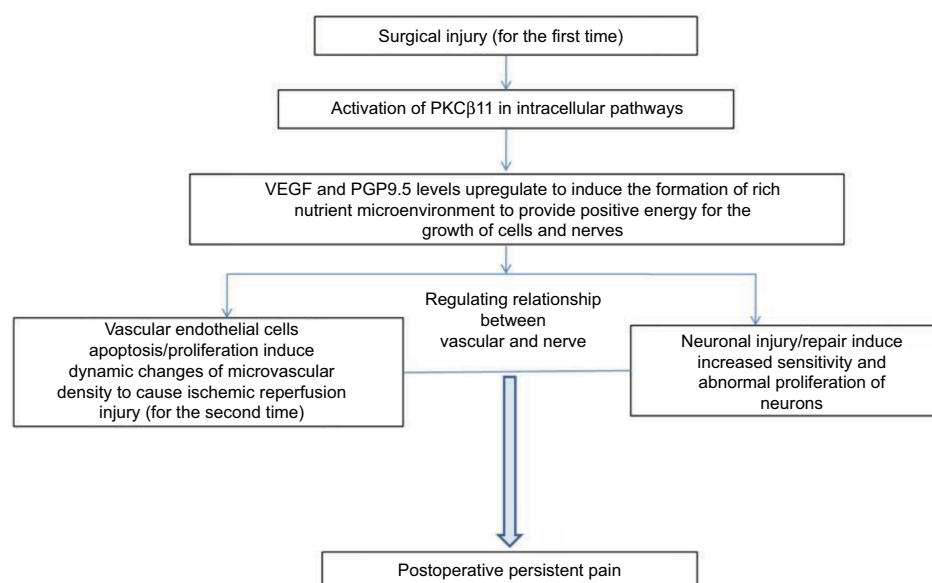

Figure 10 Schematic diagram shows potential relationships among p-PKCβII, VEGF, and PGP9.5 to cause postoperative persistent pain.
Abbreviations: VEGF, vascular endothelial growth factor; PGP, protein gene product; PKCβII, protein kinase C βII.

Acknowledgment

Disclosure

The authors report no conflicts of interest in this work.

References

1. Wang H, Heijnen CJ, van Velthoven CT, et al. Balancing GRK2 and EPAC1 levels prevents and relieves chronic pain. *J Clin Invest*. 2013;123(12):5023–5034.
2. Steinberg SF. Structural basis of protein kinase C isoform function. *Physiol Rev*. 2008;88(4):1341–1378.
3. Melemedjian OK, Tillu DV, Asiedu MN, et al. BDNF regulates atypical PKC at spinal synapses to initiate and maintain a centralized chronic pain state. *Mol Pain*. 2013;9:12.
4. Mo G, Grant R, O'Donnell D, Ragsdale DS, Cao CQ, Séguéla P. Neuropathic Nav1.3-mediated sensitization to P2X activation is regulated by protein kinase C. *Mol Pain*. 2011;7:14.
5. Roh DH, Cho SR, Yoon SY, et al. Spinal neuronal NOS activation mediates sigma-1 receptor-induced mechanical and thermal hypersensitivity in mice: involvement of PKC-dependent GluN1 phosphorylation. *Br J Pharmacol*. 2011;163(8):1707–1720.
6. Galeotti N, Farzad M, Bianchi E, Ghelardini C. PKC-mediated potentiation of morphine analgesia by St. John's Wort in rodents and humans. *J Pharmacol Sci*. 2014;124(4):409–417.
7. Mehta KD. Emerging role of protein kinase C in energy homeostasis: a brief overview. *World J Diabetes*. 2014;5(3):385–392.
8. Chen Z, Wang G, Zhai X, et al. Selective inhibition of protein kinase C beta2 attenuates the adaptor P66 Shc-mediated intestinal ischemia-reperfusion injury. *Cell Death Dis*. 2014;5:e1164.
9. Lee BK, Yoon JS, Lee MG, Jung YS. Protein kinase C-beta mediates neuronal activation of Na(+)/H(+) exchanger-1 during glutamate excitotoxicity. *Cell Signal*. 2014;26(4):697–704.
10. Wu Z, Zhao G, Peng L, et al. Protein kinase C beta mediates CD40 ligand-induced adhesion of monocytes to endothelial cells. *PLoS One*. 2013;8(9):e72593.
11. Huang YF, Liao CK, Lin JC, Jow GM, Wang HS, Wu JC. Antofine-induced connexin43 gap junction disassembly in rat astrocytes involves protein kinase Cbeta. *Neurotoxicology*. 2013;35:169–179.
12. Seoane A, Bessa X, Balleste B, et al. *Helicobacter pylori a*nd gastric cancer: relationship with histological subtype and tumor location. *Gastroenterol Hepatol*. 2005;28(2):60–64.
13. Zhao C, Leitges M, Gereau RW 4th. Isozyme-specific effects of protein kinase C in pain modulation. *Anesthesiology*. 2011;115(6):1261–1270.
14. Flatters SJ. Characterization of a model of persistent postoperative pain evoked by skin/muscle incision and retraction (SMIR). *Pain*. 2008;135(1–2):119–130.
15. Charlton E. Ethical guidelines for pain research in humans. Committee on Ethical Issues of the International Association for the Study of Pain. *Pain*. 1995;63(3):277–278.
16. Hylden JL, Wilcox GL. Intrathecal morphine in mice: a new technique. *Eur J Pharmacol*. 1980;67(2–3):313–316.
17. Dixon WJ. Staircase bioassay: the up-and-down method. *Neurosci Biobehav Rev*. 1991;15(1):47–50.
18. Manassero G, Repetto IE, Cobianchi S, et al. Role of JNK isoforms in the development of neuropathic pain following sciatic nerve transection in the mouse. *Mol Pain*. 2012;8:39.
19. Li L, Hasan R, Zhang X. The basal thermal sensitivity of the TRPV1 ion channel is determined by PKCbetaII. *J Neurosci*. 2014;34(24):8246–8258.
20. Ji RR, Berta T, Nedergaard M. Glia and pain: is chronic pain a gliopathy? *Pain*. 2013;154(Suppl 1):S10–S28.
21. Ruscheweyh R, Forsthuber L, Schoffnegger D, Sandkühler J. Modification of classical neurochemical markers in identified primary afferent neurons with Abeta-, Adelta-, and C-fibers after chronic constriction injury in mice. *J Comp Neurol*. 2007;502(2):325–336.
22. Guo A, Vulchanova L, Wang J, Li X, Elde R. Immunocytochemical localization of the vanilloid receptor 1 (VR1): relationship to neuropeptides, the P2X3 purinoceptor and IB4 binding sites. *Eur J Neurosci*. 1999;11(3):946–958.
23. Uchida K, Baba H, Maezawa Y, Kubota C. Progressive changes in neurofilament proteins and growth-associated protein-43 immunoreactivities at the site of cervical spinal cord compression in spinal hyperostotic mice. *Spine (Phila Pa 1976)*. 2002;27(5):480–486.
24. Wang G, Chen Z, Zhang F, et al. Blockade of PKCbeta protects against remote organ injury induced by intestinal ischemia and reperfusion via a p66shc-mediated mitochondrial apoptotic pathway. *Apoptosis*. 2014;19(9):1342–1353.
25. Gadad PC, Matthews KH, Knott RM. Role of HIF1alpha and PKCbeta in mediating the effect of oxygen and glucose in a novel wound assay. *Microvasc Res*. 2013;88:61–69.
26. Tanaka R, Miwa Y, Mou K, et al. Knockout of the l-pgds gene aggravates obesity and atherosclerosis in mice. *Biochem Biophys Res Commun*. 2009;378(4):851–856.
27. Zevallos HB, McKinnon B, Tokushige N, Mueller MD, Fraser IS, Bersinger NA. Detection of the pan neuronal marker PGP9.5 by immuno-histochemistry and quantitative PCR in eutopic endometrium from women with and without endometriosis. *Arch Gynecol Obstet*. 2015;291(1):85–91.
28. Shirai C, Ohtori S, Kishida S, Harada Y, Moriya H, et al. The pattern of distribution of PGP 9.5 and TNF-alpha immunoreactive sensory nerve fibers in the labrum and synovium of the human hip joint. *Neurosci Lett*. 2009;450(1):18–22.
29. Kosacka J, Nowicki M, Blüher M, et al. Increased autophagy in peripheral nerves may protect Wistar Ottawa Karlsburg W rats against neuropathy. *Exp Neurol*. 2013;250:125–135.
30. Liu BL, Yang F, Zhan HL, et al. Increased severity of inflammation correlates with elevated expression of TRPV1 nerve fibers and nerve growth factor on interstitial cystitis/bladder pain syndrome. *Urol Int*. 2014;92(2):202–208.
31. Del Fiacco M, Quartu M, Boi M, et al. TRPV1, CGRP and SP in scalp arteries of patients suffering from chronic migraine. *J Neurol Neurosurg Psychiatry*. 2015;86(4):393–397.
32. Giordano C, Siniscalco D, Melisi D, et al. The galactosylation of N(omega)-nitro-L-arginine enhances its anti-nocifensive or anti-allodynic effects by targeting glia in healthy and neuropathic mice. *Eur J Pharmacol*. 2011;656(1–3):52–62.
33. Koyama J, Miyake S, Sasayama T, Chiba Y, Kondoh T, Kohmura E. The novel VEGF receptor antagonist, VGA1155, reduces edema, decreases infarct and improves neurological function after stroke in rats. *Kobe J Med Sci*. 2010;56(1):E1–E11.
34. Sone H, Deo BK, Kumagai AK. Enhancement of glucose transport by vascular endothelial growth factor in retinal endothelial cells. *Invest Ophthalmol Vis Sci*. 2000;41(7):1876–1884.
35. Bry M, Kivelä R, Leppänen VM, Alitalo K. *V*ascular endothelial growth factor-B in physiology and disease. *Physiol Rev*. 2014;94(3):779–794.
36. Bespalov AG, Tregub PP, Kulikov VP, Pijanzin AI, Belousov AA. [The role of VEGF, HSP-70 and protein S-100B in the potentiation effect of the neuroprotective effect of hypercapnic hypoxia]. *Patol Fiziol Eksp Ter*. 2014;2:24–27. Russian.
37. Murakami K, Kuniyoshi K, Iwakura N, et al. Vein wrapping for chronic nerve constriction injury in a rat model: study showing increases in VEGF and HGF production and prevention of pain-associated behaviors and nerve damage. *J Bone Joint Surg Am*. 2014;96(10):859–867.